Noninvasive monitoring of photodynamic therapy on skin neoplastic lesions using the optical attenuation coefficient measured by optical coherence tomography

Viviane P. Goulart
Moisés O. dos Santos
Anne Latrive
Anderson Z. Freitas
Luciana Correa
Denise M. Zezell

SPIE.

Noninvasive monitoring of photodynamic therapy on skin neoplastic lesions using the optical attenuation coefficient measured by optical coherence tomography

Viviane P. Goulart,[a] Moisés O. dos Santos,[b] Anne Latrive,[a] Anderson Z. Freitas,[a] Luciana Correa,[c] and Denise M. Zezell[a,*]

[a]IPEN-CNEN/SP, Center for Lasers and Applications—CLA, Laboratório de Biofotônica, Av. Prof. Lineu Prestes, 2242, São Paulo, 05508-000, SP, Brazil
[b]Universidade do Estado do Amazonas, Escola Superior de Tecnologia, Av. Darcy Vargas, 1200, Parque 10 de Novembro, Manaus, 69050-020, AM, Brazil
[c]Universidade de Sao Paulo, Faculdade de Odontologia, Av. Lineu Prestes, 2227, Sao Paulo, 05508-000, SP, Brazil

Abstract. Photodynamic therapy (PDT) has become a promising alternative for treatment of skin lesions such as squamous cell carcinoma. We propose a method to monitor the effects of PDT in a noninvasive way by using the optical attenuation coefficient (OAC) calculated from optical coherence tomography (OCT) images. We conducted a study on mice with chemically induced neoplastic lesions and performed PDT on these lesions using homemade photosensitizers. The response of neoplastic lesions to therapy was monitored using, at the same time, macroscopic clinical visualization, histopathological analysis, OCT imaging, and OCT-based attenuation coefficient measurement. Results with all four modalities demonstrated a positive response to treatment. The attenuation coefficient was found to be 1.4 higher in skin lesions than in healthy tissue and it decreased after therapy. This study shows that the OAC is a potential tool to noninvasively assess the evolution of skin neoplastic lesions with time after treatment. © 2015 Society of Photo-Optical Instrumentation Engineers (SPIE) [DOI: 10.1117/1.JBO.20.5.051007]

1 Introduction

Squamous cells carcinoma (SCC) in the skin are malignant neoplastic lesions with a substantial risk of metastasis.[1] They are most commonly found on the head and neck areas and are mainly caused by exposure to mutation-inducing chemical agents or ultraviolet radiation. Because of lifestyle changes and greater sun exposure, the incidence of SCC has significantly increased over the past decades.[2] The main classical treatments include chemo- or radiotherapy, cryotherapy, curettage, surgical excision or Mohs' surgery, with a high rate of cure. However, these treatments usually require large marginal areas which can be disfiguring for the patient. A noninvasive alternative option with excellent cosmetic results is photodynamic therapy (PDT).

In a few decades, PDT has evolved from an experimental therapy for a variety of human cancers to a common tool for the treatment of skin lesions such as actinic keratosis or basal cell carcinoma.[3] The principle of PDT is to topically apply on the lesion a nontoxic photosensitizer (PS) that will specifically accumulate inside the cells to be eliminated, then to irradiate the tissue with light at a specific wavelength. The energy of the incoming light is absorbed by the PS and leads to the production of highly reactive oxygen species that will induce necrosis and cell apoptosis. The type and concentration of PS, the light dose, and the time interval between the application of the PS and light irradiation are obviously crucial parameters for PDT efficacy. Although PDT has achieved great progress since its beginning, there are still some limitations to overcome such as irradiation distribution, tissue oxygen consumption, or the heterogeneous PS concentration.[4] Therefore, there is a need for further optimization studies which requires noninvasive monitoring of tumor evolution during PDT.

Optical coherence tomography (OCT) is a high-resolution optical imaging technique that performs depth-resolved microscopy of tissue based on the principle of low-coherence interferometry.[5] The sample is illuminated with a broadband low-coherence source such as a laser or even a halogen at wavelengths between 700 and 1300 nm. The detector receives the light backscattered by the microscopic features of the sample. The depth information on the signal is then given by the interferences produced in combination with a reference arm.

Since its development in the early 1990s, OCT has mainly been used in ophthalmology, but it is also a promising new method for the investigation of skin morphology.[6–9] Its diagnostic ability has already been proven for nonmelanoma skin cancers.[10–13] Since OCT imaging is performed in real time in a noninvasive way and with no side effects, it is a well-suited tool for *in vivo* disease monitoring. Furthermore, additional information, such as the tissue refractive index or optical attenuation coefficient (OAC), can be extracted from the raw backscattering OCT images.[14–17]

---

*Address all correspondence to: Denise M. Zezell, E-mail: zezell@usp.br

Table 1 Mice groups.

Group	Number of mice	Description
G1	3	Healthy skin
G2	10	Neoplastic tissue
G3	5	Neoplastic tissue + ALA + PDT
G4	5	Neoplastic tissue + MEALA + PDT

We propose the use of the imaging technique of OCT and the subsequent measurement of the OAC to optically characterize the tissue and evolution of SCC during PDT, and eventually as a marker of PDT efficacy.

2 Materials and Methods

2.1 Chemical Carcinogenesis

For our study, we chose a well-established *in vivo* model of chemically induced skin tumor on mice.[18] We used 50 Swiss breed female mice, aged from 8 to 10 weeks, with a weight of 20 g. The animals were anesthetized with ketamine (0.35 ml/kg) and xylazine (0.20 ml/kg) during all stages of the protocol, which was approved by the ethics committee for research on animals of IPEN (No. 71/10-CEUA-IPEN/SP).

The mice were divided into four groups (Table 1). The chemical carcinogenesis consisted of two stages. The initiation phase was a topical application of 50-mg 7,12-dimethyl benzanthracene (DMBA) diluted in 100 mL of acetone on the shaved backs of the mice. The promotion phase begins 1 week after and consists of a biweekly application of 5 g of 12-O-tetradecanoylphorbol-13 acetate (TPA) diluted in 200 ml of acetone for 28 weeks. After 28 weeks, the animals obtained visible single or multiple tumor nodules with verrucous aspect (Fig. 1). The control group only received a topical application of acetone.

A standard protocol was established to photograph the induced lesions at the different stages of the treatment in order to precisely follow their size evolution.

Considering the histopathological evaluation as the gold standard, we analyzed the histological profiles of healthy and tumorous mouse skin. We performed excisional biopsies of each papilomatous lesion with a size of about 0.5 to 1.0 cm. The collection was done immediately before PDT, at 10 days, and at 20 days after PDT. The histopathological analysis was performed by a pathologist. We can clearly see the differences between both tissues on Fig. 2. Healthy skin epidermis has

three to four cell layers and a thin layer of keratin. The dermis is composed of dense connective tissue, clear hair follicles, and organized hypodermis. Neoplastic lesions show an intense proliferation of keratinocytes in an exophytic pattern [Fig. 2(b)]. The basal layer epithelium displays a moderate dysplasia and hyperchromatism. Hyperkeratosis and papillary projections were frequently observed. Twenty-five rats exhibited several lesions with a histological pattern clearly indicating SCC, with invasion of the neoplastic cells into the dermis, intense collagen deposition, and numerous blood vessels. In the remaining cases, neoplastic invasion was not evident, but the lesions were considered as potentially malignant tumors due to the dysplastic pattern present in all the cases. The lesions' thicknesses vary from 200 to 500 μm. The majority exhibited invasion in a depth restricted up to 300 μm.

2.2 Photodynamic Therapy

For PDT, we used homemade PS ointments. The base is prepared with lanolin and petrolatum, the active principle being either aminolevulinic acid (ALA) (20%) or aminolevulinic methyl ester (MEALA) (10%), and the other ingredients are kept confidential (patent pending PI N°0705591-9).[19] The ointment was applied on the tumor lesions with a 5-mm additional margin, for each 30 min during a 5 h period, and the excess was removed with a gauze before PDT. Light irradiation was performed with a prototype of cluster of LEDs at 630 nm (power 180 mW, power density 5 mW/cm^2). We performed one session of PDT during which the lesions were irradiated for 40 min with an energy density of 12 J/cm^2.

Table 1 shows the different treatments applied to the four mice groups. Only 23 animals were further evaluated in our study due to a high death rate of 54%. This death rate is expected due to the toxicity of DMBA/TPA and is in agreement with other studies.[18]

2.3 Optical Coherence Tomography Imaging

Analyses by optical coherence tomography were performed immediately before the PDT and at 10 and 20 days after PDT. OCT is a real-time technique so that the whole imaging protocol lasted less than 30 min. The commercial OCT system used in this study is an OCP930SR (Thorlabs Inc., USA; Fig. 3). It has a superluminescent diode source with a central wavelength of 930 nm and a bandwidth of 100 nm. Optical axial resolution was calculated at 4.38 μm, after refraction index correction ($n = 1.41$ at 930 nm), and a lateral resolution at 6.1 μm. The images have dimensions of 1000×512 pixels,

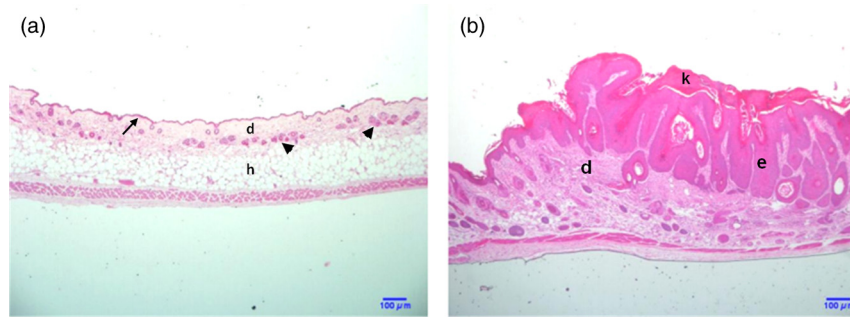**Fig. 1** Macroscopic view of the skin lesions.

Fig. 2 Light microscopy of representative histological sections. (a) Healthy skin of control group, (b) neoplastic lesion with exophytic pattern *e* and intense keratinization *k*. Arrow—normal epithelium; head arrow—hair follicle; d—dermis; h—hypodermis (hematoxylin and eosin, original magnification with 4× objective).

corresponding to a lateral field of 5.0 mm and a depth field of 1.5 mm.

2.4 *Optical Attenuation Coefficient Measurement*

Two types of models exist for the OCT signal, depending on whether only single scattering or multiple scattering is considered.[20] In our case, we used a simple model of exponential decay of the backscattered light, according to the following equation:

$$I(z) = I_0 e^{-2\alpha z} + C \tag{1}$$

where I represents the value of the detected intensity, I_0 is the intensity of incident light, α is the OAC (total OAC integrated over the whole depth), z is the depth of analysis, and C is a constant for background noise.

Analysis was performed through a LabView software developed in our laboratory. The decay profile of each A-line $I(z)$ is fitted by an exponential curve to obtain a local estimation of the OAC. A global OAC for each image is obtained as the arithmetic mean over all selected A-lines. Indeed, the program allows selecting a region of interest in the lateral and axial dimensions, facilitating the location of tumoral epithelium and dermis and the exclusion of objects such as the hair follicles that could interfere with the optical signal.
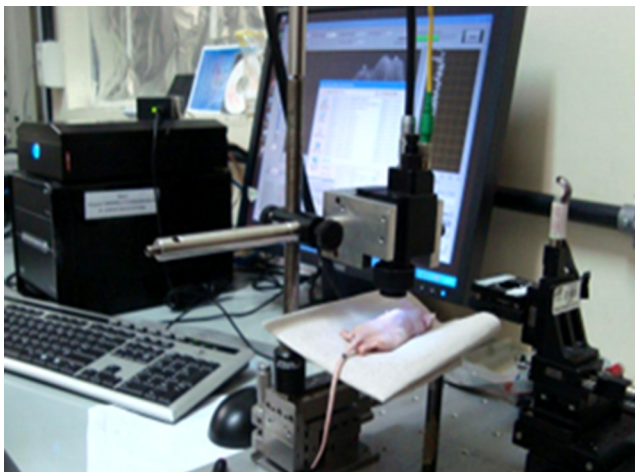

Fig. 3 OCT imaging on anesthetized mouse.

3 Results

3.1 *Clinical Evaluation of PDT Through Macroscopic Images and Histopathological Analysis*

Clinical signs of the PDT effect were observed at 24 h after the treatment. The treated lesions exhibited a superficial necrosis and/or crust. At 10 and 20 days, the lesions' sizes had diminished and the superficial crust had disappeared. The effect of PDT treatment on groups G3 and G4 was macroscopically assessed by the evolution of the area of each lesions, measured using ImageJ software. Figure 4 shows the frequency of the lesions depending on their percentage of area reduction. After 20 days, all lesions showed a positive response to PDT, ranking from a slight decrease (25%) to total disappearance (100%).

Globally, we can see a decrease in the total area of the lesions after PDT (Fig. 5). Normalization and variance homogenization of the data were performed using the Shapiro–Wilk and Bartlett's test at a level of significance of 5%. Then statistical analysis of variance (ANOVA, 5%) and comparison of G3 and G4 using the Tukey–Kramer test (5%) demonstrated that there is no significant difference between G3 and G4 in any of the periods. The larger error bar in group G3 at day 20 after PDT is due to the loss of an animal during this time interval due to the aggressiveness of the tumor, which reduced the total number of evaluated lesions and might have influenced the outcome for group G3.

Representative samples from groups G3 and G4 were further subjected to histopathological analysis (Fig. 6). After 10 days of PDT, in G3 there was an evident reduction of the epithelium thickness [Fig. 6(a)], and in G4, ulceration and extensive epithelial necrosis were present [Fig. 6(c)]. At 20 days post-PDT, the papillary pattern was not visible in G3 [Fig. 6(b)] and the connective tissue exhibited intense reparative process. In G4, in the same experimental period, numerous fibroblasts and marked extracellular matrix deposition were observed accompanied with reduction of the epithelium thickness [Fig. 6(d)]. In some cases of G3 and G4 (about 15%), there was no sign of neoplastic cells. Total reepithelization and remodeling of the epithelial layers were evident. Fibrous connective tissue and regeneration of the hair follicles were observed in the dermis.

Based on these clinical and histopathological evaluations, we can conclude that there is a significant reduction in neoplastic lesions after 20 days of PDT treatment.
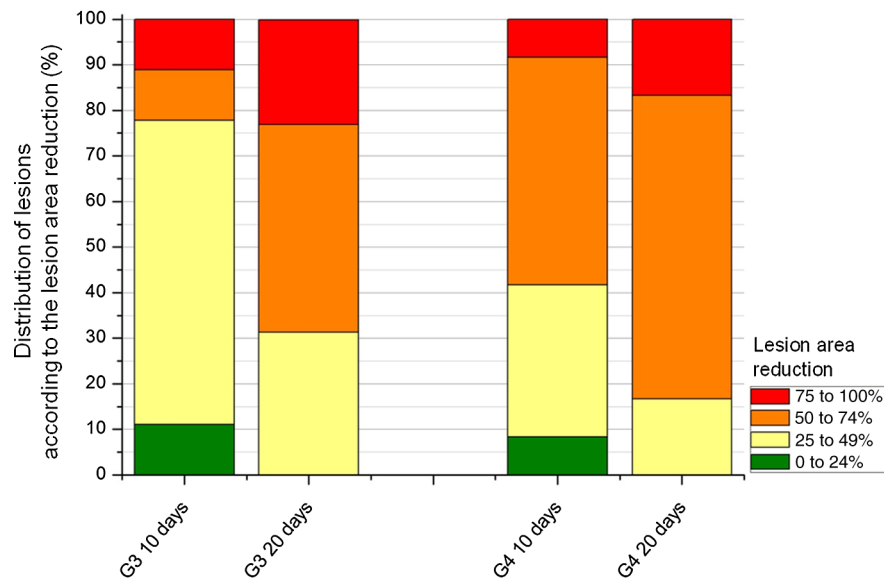
Fig. 4 Evolution of the area of each lesion. Number of lesions in each class (area reduction between 0% and 24%, 25% and 49%, 50% and 74%, or 75% and 100%) for G3 and G4, 10 and 20 days after PDT.

3.2 Optical Coherence Tomography Imaging

For each study group, we obtained OCT images and OAC estimation. Figure 7 shows the representative OCT images of healthy and neoplastic skins. The red arrows point to epithelium which is thin in healthy skin and becomes thick with cells in neoplastic tissue, suggesting epithelial hyperplasia.

3.3 Optical Attenuation Coefficient Evolution

To evaluate the efficacy of PDT, we chose the OAC of healthy skin as the standard to achieve: the closer the OAC is to of that of healthy skin, the better the effect of PDT is.

The OAC measurement using the whole depth of OCT images, from 0 to 1 mm, did not show any difference between healthy and neoplastic tissues. This is due to the fact that the signal from this region is strongly influenced by deeper regions
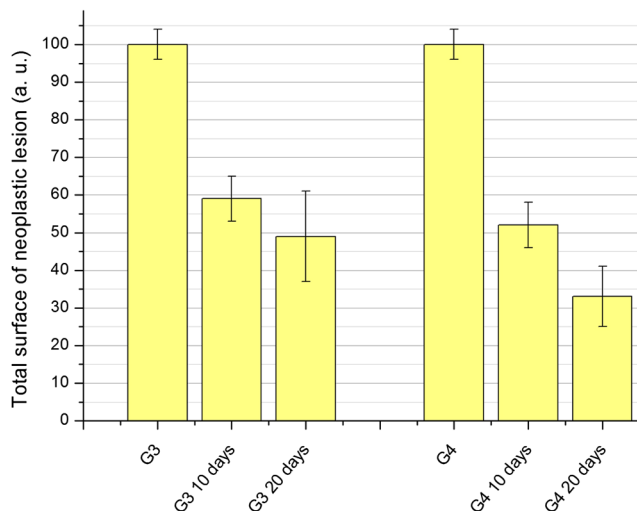

Fig. 5 Evolution of the total area of the neoplastic lesions for G3 (ALA-mediated PDT) and G4 (MEALA-mediated PDT), 10 and 20 days after PDT.

of the hypodermis which are not affected by tumor. Thus, we chose to analyze the data of the OCT images at restricted depths from 10 to 300 μm. This depth range ignores the contribution of non-neoplastic signal and is the representative of changes associated with neoplastic lesions. It is also consistent with the depth of SCC lesions evaluated between 200 and 500 μm by histology.

Figure 8 shows the mean OAC of groups G2, G3, and G4, normalized by the OAC of control group G1.

As before, normalization and variance homogenization of the data were performed using the Shapiro-Wilk and Bartlett's test (5%), then statistical ANOVA (5%) and comparison using the Tukey–Kramer test (5%) demonstrated that there is significant difference between the groups.

The OAC of neoplastic tissue (G2) is greater than the OAC of healthy skin (G1) by a factor of around 1.4. The OAC of neoplastic tissue in G3 and G4 subjected to PDT tends to approach that of healthy tissue at 10 days after treatment, showing a positive response to treatment.

The OAC of G3 increases from 10 to 20 days after PDT with statistical significance, which is not in agreement with the clinical outcome. This increase is also observed for G4, but without statistical significance. This can be because the OAC measurement was influenced by the backscattering signal from hair follicles. The histological slides at day 20 showed the regeneration of hair follicles, which is greater in group G3 than G4 [Figs. 6(b) and 6(d)]. Group G4 presents fewer hair follicles due to more intense fibrosis that develops in the scar tissue of the dermis. This fibrosis could also be responsible for an increase in the OAC of group G4.

4 Discussion

The model of chemical carcinogenesis carried out for this study was very effective in mimicking the induction and progression of malignant tumors in skin. The disadvantage of this model is the long induction time and the high loss rate (54%) caused by the poor state of the animals during the 31 weeks of the experiment, thereby reducing the number of samples of the study.

DMBA-induced neoplastic lesions in skin are characterized by the presence of papilloma with moderate to intense epithelial
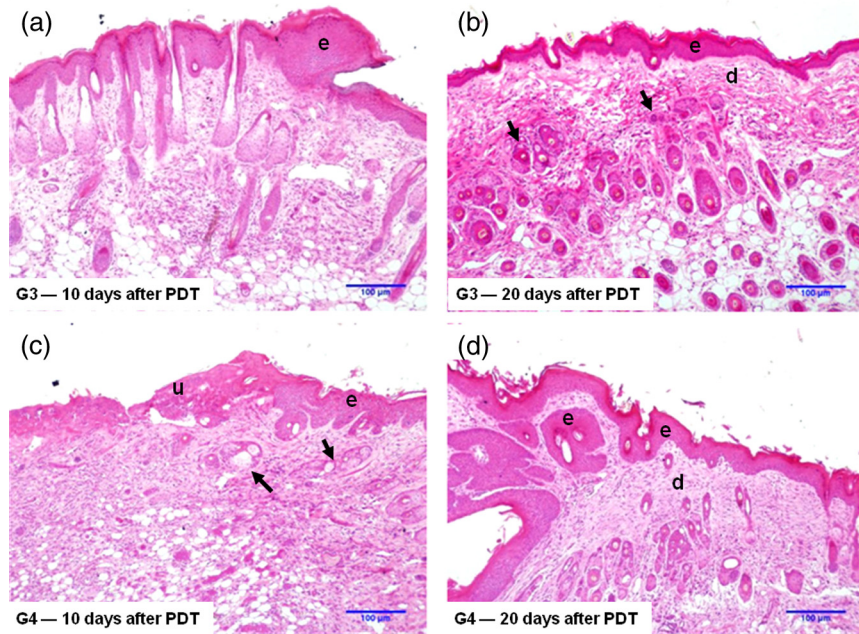
Fig. 6 Light microscopy of representative histological sections. (a) Reduction of epithelium thickness *e* at 10 days after PDT in G3 when compared with the initial aspect observed at Fig. 2(b). (b) Reduction of epithelium thickness *e* is marked at 20 days after PDT. The dermis *d* exhibits intense collagenization and hair follicles (arrow) are in regenerative process. (c) Ulceration *u* of epithelium *e* and necrosis of hair follicles (arrows) at 10 days after PDT in G4. (d) After 20 days in this group, reepithelization, reduction of exophytic pattern of the tumor *e*, and increase on cellularity and collagenization in dermis *d* are evident, indicating an advanced reparative process (hematoxylin and eosin, original magnification with 10× objective).

atypia. These lesions can progress to invasive epithelial cords surrounded by inflammatory cells. Cellular and morphological changes were assessed using, at the same time, visual macroscopic inspection, gold-standard histopathological analysis, and OCT imaging. A unique approach of this study is to further

evaluate the response of the tumorous lesions to PDT using the OAC extracted from the OCT signal, an optical property without previous description in literature for tumorous skin tissue. We measured the OAC using a simple single-scattering model and considering a precisely delimited range of depths in the OCT signal. The histological images were mainly used to diagnose the lesion and to obtain the thicknesses of the hyperplasic epithelium and dermis. The selection of the region of interest for
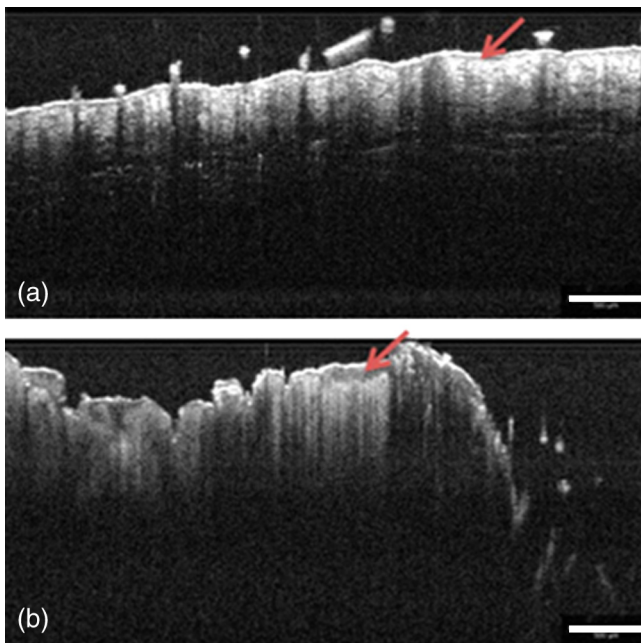

Fig. 7 OCT images on skin of (a) healthy and (b) neoplastic tissues. The red arrows indicate the epithelium, which is thin in (a) and thick in (b). Scale bar 500 μm.
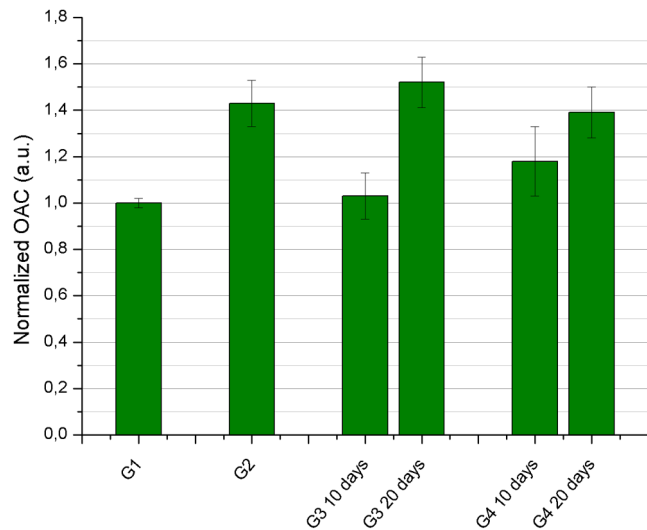

Fig. 8 Optical attenuation coefficient (OAC) calculated for depths from 10 to 300 μm. G1: normal skin; G2: skin with neoplastic lesions; G3: neoplastic lesions treated with ALA-mediated PDT; G4: neoplastic lesions treated with MEALA-induced PDT.

calculation of the OAC was then done manually by the observer. We found that the morphological characteristics of the OCT image were enough to guide the observer to delimitate the region of interest. In the present study, it was essential to correctly choose the region of interest and depth range relevant for OAC analysis to ensure that only the tumor signal is used for computation, avoiding the keratin layer and subcutaneous tissue. Moreover, a previous study on burn scar tissue showed that the signal from blood vessels inside the dermis can interfere with OAC measurement.[21] We ensured that no large blood vessels were present on the OCT images before each OAC computation by visual inspection, although unresolved capillaries may still be present.

We found that the OAC of neoplastic tissue was 1.4 times higher than that of healthy skin. This can be optically explained by the hyperkeratosis and greater number of epithelial cells present in the tumor. These cells were organized in multiple layers that composed a dense and more keratinized epidermis, increasing the attenuation of light. Moreover, tissue disorganization in tumor increases the number of optical interfaces inside the tissue and thus light scattering. We observed a decrease in OAC 10 days after PDT, showing the efficacy of the treatment which was compatible with histopathological findings. In fact, the ulceration present at 10 days after PDT indicates a drastic reduction of the epithelial layers' thickness. Additionally, at this time, the connective tissue in the dermis showed an extracellular matrix composed of thin fibers. Both of these microscopic aspects may explain the OAC decrease in PDT groups at 10 days.

The efficacy of the treatment was detected by the reduction of the area lesions observed clinically and by the clear necrosis of the neoplastic tissue. These differences were also detected in OAC.

To the best of our knowledge, there is currently no other study evaluating the OAC for diagnosis or tumor treatment efficacy on skin. We can only qualitatively compare our results with one other report on sunlight exposed skin.[22] It showed that the actinic keratosis lesions had higher OCT signal attenuation than healthy skin due to hyperkeratosis and a higher number of cells in dysplastic lesions, in agreement with our findings.

We have shown that the OAC will not necessarily follow a decreasing curve after treatment, but that it can exhibit phases of decrease and increase following the development of novel structures such as hair follicles or of fibrosis. Thus, establishing a direct correlation between a clinical state of the tumor and a particular valor OAC can be delicate, as has also been shown in other works.[23] However, the phases of OAC evolution can give valuable information on the phases of skin reconstruction at a microscopic scale. Further studies with more samples and with more time points would improve the precision and statistical significance of the results.

5 Conclusion

In our study, we performed chemical induction of cutaneous neoplastic lesions in mice which were treated with PDT using ALA- or MEALA-based PSs. We monitored the efficacy of PDT using clinical inspection, histological analysis, OCT imaging, and OAC measurement. We showed that the neoplastic lesions exhibited higher OAC than healthy skin and detected an OAC modification after PDT that was compatible with clinical and histological findings.

Analysis of OAC is novel and requires a precise delimitation of the region of interest, as is the case of many imaging modalities. We believe that this optical property could provide relevant information about the differences between neoplastic and healthy human and animal tissues. Moreover, its noninvasiveness makes it a promising tool for the diagnosis of skin lesions and monitoring of therapy. More studies are necessary to evaluate the sensibility and specificity of this method in skin tumor detection and prognosis.

References

1. M. Alam and D. Ratner, "Cutaneous squamous-cell carcinoma," *N. Engl. J. Med.* **344**(13), 975–983 (2001).
2. R. P. Gallagher et al., "Sunlight exposure, pigmentation factors, and risk of nonmelanocytic skin cancer: II. squamous cell carcinoma," *Arch. Dermatol.* **131**(2), 164–169 (1995).
3. P. Babilas, M. Landthaler, and R. Szeimies, "Photodynamic therapy in dermatology," *Eur. J. Dermatol.* **16**, 340–348 (2006).
4. S. H. Ibbotson, "An overview of topical photodynamic therapy in dermatology," *Photodiagn. Photodyn. Ther.* **7**(1), 16–23 (2010).
5. D. Huang et al., "Optical coherence tomography," *Science* **254**, 1178–1181 (1991).
6. J. Welzel, "Optical coherence tomography in dermatology: a review," *Skin Res. Technol.* **7**, 1–9 (2001).
7. E. Sattler, R. Kästle, and J. Welzel, "Optical coherence tomography in dermatology," *J. Biomed. Opt.* **18**(6), 061224 (2013).
8. N. D. Gladkova et al., "*In vivo* optical coherence tomography imaging of human skin: norm and pathology," *Skin Res. Technol.* **6**(1), 6–16 (2000).
9. A. Kokolakis et al., "Prehistological evaluation of benign and malignant pigmented skin lesions with optical computed tomography," *J. Biomed. Opt.* **17**(6), 066004 (2012).
10. K.-S. Lee et al., "Three-dimensional imaging of normal skin and nonmelanoma skin cancer with cellular resolution using Gabor domain optical coherence microscopy," *J. Biomed. Opt.* **17**(12), 126006 (2012).
11. Y.-C. Ahn et al., "Multimodality approach to optical early detection and mapping of oral neoplasia," *J. Biomed. Opt.* **16**(7), 076007 (2011).
12. A. Alex et al., "3D optical coherence tomography for clinical diagnosis of nonmelanoma skin cancers," *Imaging Med.* **3**(6), 653–674 (2011).
13. P. Wilder-Smith et al., "In vivo optical coherence tomography for the diagnosis of oral malignancy," *Lasers Surg. Med.* **35**(4), 269–275 (2004).
14. D. J. Faber et al., "Quantitative measurement of attenuation coefficients of weakly scattering media using optical coherence tomography," *Opt. Express* **12**(19), 590–592 (2004).
15. A. I. Kholodnykh et al., "Accurate measurement of total attenuation coefficient of thin tissue with optical coherence tomography," *IEEE J. Sel. Top. Quantum Electron.* **9**(2), 210–221 (2003).
16. D. P. Popescu et al., "Assessment of early demineralization in teeth using the signal attenuation in optical coherence tomography images," *J. Biomed. Opt.* **13**(5), 054053 (2008).
17. C. H. Wilder-Smith et al., "Quantification of dental erosions in patients with GERD using optical coherence tomography before and after double-blind, randomized treatment with esomeprazole or placebo," *Am. J. Gastroenterol.* **104**(11), 2788–2795 (2009).
18. E. L. Abel et al., "Multi-stage chemical carcinogenesis in mouse skin: fundamentals and applications," *Nat. Protoc.* **4**(9), 1350–1362 (2009).
19. R. F. Donnelly et al., "Influence of formulation factors on methyl-ALA-induced protoporphyrin IX accumulation *in vivo*," *Photodiagn. Photodyn. Ther.* **3**(3), 190–201 (2006).

20. L. Thrane, H. T. Yura, and P. E. Andersen, "Analysis of optical coherence tomography systems based on the extended Huygens Fresnel principle," *J. Opt. Soc. Am. A* **17**(3), 484–490 (2000).
21. P. Gong et al., "Assessment of human burn scars with optical coherence tomography by imaging the attenuation coefficient of tissue after vascular masking," *J. Biomed. Opt.* **19**(2), 021111 (2013).
22. V. R. Korde et al., "Using optical coherence tomography to evaluate skin sun damage and precancer," *Lasers Surg. Med.* **39**(9), 687–695 (2007).
23. E. C. C. Cauberg et al., "Quantitative measurement of attenuation coefficients of bladder biopsies using optical coherence tomography for grading urothelial carcinoma of the bladder," *J. Biomed. Opt.* **15**(6), 066013 (2010).

Viviane P. Goulart graduated in biological science and received her MSc degree in nuclear technology of materials from the University of São Paulo, Brazil. Her studies cover the field of histology, OCT, and fluorescence spectroscopy.

Moisés O. dos Santos received his MSc degree in physics applied to medicine and biology and PhD degree in nuclear technology—material from the University of São Paulo, Brazil. His studies cover the field of instrumentation, histology, OCT, nonlinear imaging (second harmonic generation and two-photon emission fluorescence microscope), and infrared spectroscopy. Since 2014, he has been an assistant professor of physics at the State University of Amazonas.

Anne Latrive is a postdoctorate researcher at IPEN, São Paulo, working with Prof. Denise M. Zezell on OCT medical applications. She was previously a project manager at LLTech responsible for developing novel endoscopic OCT devices. She conducted her PhD with Prof. Claude Boccara at Langevin Institute, Paris, on full-field OCT for endoscopy. She has an engineering degree from Ecole Centrale Paris Graduate School and an MSc degree in biophysics of Pierre and Marie Curie University in Paris.

Anderson Z. Freitas graduated in physics and got his Msc and PhD degrees in science at the University of São Paulo, Brazil. He is currently a researcher at the Center for Lasers and Applications of IPEN—CNEN/SP in the areas of optical diagnostic methods, mainly OCT for dermatology, odontology, and cosmetology.

Luciana Correa is an associate professor in the General Pathology Department in the School of Dentistry, University of São Paulo. She is responsible for the Laboratory of Experimental Pathology, focused on the development of animal models for the study of carcinogenesis and immunosuppression. The study of molecular events associated with activation of heat shock proteins and cellular death cascade after phototherapies is one of her main research lines.

Denise M. Zezell is a senior researcher at Center for Lasers and Applications and vice dean of graduation at IPEN—CNEN-SP/ University of São Paulo. From 1999 to 2012, she was the head of the master course in lasers in dentistry. She is responsible for the Laboratory of Biophotonics at IPEN—CNEN-SP, developing new diagnosis and therapeutic methods based in photonics. Present interests include also micro-FTIR and spectral imaging in the characterization of biological tissues and diagnosis of cancer.